

Pregeometric Origins of Liquidity Geometry in Financial Order Books

João P. da Cruz

*The Quantum Computer Company, Lisbon, Portugal** and
Center for Theoretical and Computational Physics, Lisbon, Portugal

(Dated: January 27, 2026)

We propose a structural framework for the geometry of financial order books in which liquidity, supply, and demand are treated as emergent observables rather than primitive economic variables. The market is modeled as an inflationary relational system without assumed metric, temporal, or price coordinates. Observable quantities arise only through projection, implemented here via spectral embeddings of the graph Laplacian. A one-dimensional projection induces a price-like coordinate, while the projected density defines liquidity profiles around the mid price. Under a minimal single-scale hypothesis—excluding intrinsic length scales beyond distance to the mid and finite visibility—we show that projected supply and demand are constrained to gamma-like functional forms. In discrete data, this prediction translates into integrated-gamma cumulative profiles. We test these results using high-frequency Level II data for several U.S. equities and find robust agreement across assets and intraday windows. Explicit comparison with alternative cumulative models using information criteria demonstrates a systematic preference for the integrated-gamma geometry. A minimal simulation of inflationary relational dynamics reproduces the same structure without invoking agent behavior or price formation mechanisms. These results indicate that key regularities of order-book liquidity reflect geometric constraints induced by observation rather than detailed microstructural dynamics.

I. INTRODUCTION

Financial markets are commonly described in terms of prices evolving in time, with supply and demand curves interpreted as behavioral responses of trading agents. In this view, order books encode strategic intentions, information asymmetries, and equilibrium-seeking dynamics. Despite the diversity of such models, empirical studies of high-frequency data have repeatedly documented robust structural regularities in order-book liquidity, including convex profiles near the mid price, heavy tails, and scale-dependent decay [13, 15, 16]. The origin of these regularities, however, remains debated.

Most existing approaches treat price and time as fundamental variables and seek to explain observed order-book shapes through explicit microstructural mechanisms, such as order placement strategies, inventory control, or market impact. Agent-based and stochastic models have been particularly successful in this respect. Notably, the model introduced by Mike and Farmer [14] demonstrated that heavy-tailed order placement and cancellation processes are sufficient to generate realistic order-book shapes and price diffusion. Similarly, Cont, Stoikov, and Talreja [17] proposed a queue-reactive framework in which liquidity profiles emerge from the interaction of stochastic order flows at discrete price levels. While these models reproduce many empirical features, they rely on behavioral assumptions, calibration choices, or equilibrium concepts whose universality across assets and market conditions is difficult to establish.

In this work, we adopt a complementary perspective. Rather than modeling price formation directly or specify-

ing microscopic order flow mechanisms, we ask whether familiar order-book observables can emerge generically from the projection of a more primitive relational structure. Our approach is inspired by pregeometric frameworks in statistical physics, where geometry and dynamics are not assumed at the microscopic level but arise only through observation and coarse-graining.

We model the market as an inflationary relational network whose fundamental description contains no metric, temporal ordering, or economic coordinates. Vertices represent abstract economic entities, and edges encode the possibility of interaction. Growth and reorganization proceed through inflationary updates that generate heterogeneous, hub-dominated structures without fine-tuning. Crucially, none of the standard market observables are defined at this level.

Observable quantities arise only through projection. By applying spectral embeddings based on the graph Laplacian, an observer assigns effective coordinates to the relational substrate. A one-dimensional projection induces a scalar coordinate naturally interpreted as price, while the distribution of projected density defines liquidity profiles. Successive projections of an evolving relational system give rise to apparent time series, returns, and fluctuations, even though no fundamental time variable exists microscopically.

Within this framework, supply and demand are not independent behavioral curves but geometric branches of a single projected density. We show that, under minimal structural assumptions on regularity, vanishing liquidity at the mid, and exponential decay at large distances, the projected liquidity profiles necessarily adopt a gamma-like functional form. This result is structural and geometric in nature, and does not rely on equilibrium arguments, optimization principles, or agent-level behavior.

* joao@quantumcomp.pt

We test these ideas empirically using high-frequency Level II data for several U.S. equities across different sectors. By focusing on short time windows, we extract instantaneous liquidity profiles relative to the mid price and show that their cumulative forms are well described by integrated gamma functions. The fitted parameters vary across assets and windows, indicating that they characterize local projected geometry rather than stationary market states. A minimal simulation of inflationary relational dynamics reproduces the same functional structure in the absence of any market-specific assumptions.

The goal of this work is not predictive. Instead, it is to demonstrate that standard order-book regularities can be understood as emergent geometric observables induced by projection. This perspective shifts the modeling focus from price dynamics to the geometry of observation and provides a unifying structural interpretation of liquidity in financial markets.

II. RELATIONAL INFLATIONARY MODEL

We introduce a minimal relational framework aimed at understanding how market observables arise without assuming price, time, return, or risk as primitive variables. The construction is deliberately *pregeometric*: no metric, ordering, or economic coordinate is postulated at the microscopic level. All quantities conventionally used to describe markets will be shown to emerge only through observation.

A. Relational substrate

The system is defined by a growing graph $G = (V, E)$, where vertices represent economic entities (agents, venues, or abstract trading units) and edges encode the possibility of interaction or exchange. At this level, the graph is purely combinatorial: it carries no spatial embedding, no weights, and no intrinsic notion of distance.

The only primitive object is adjacency. In particular, there is no distinguished notion of price, time, or volume attached to vertices or edges. Observable quantities will be defined *a posteriori* through projection.

B. Inflationary dynamics

The relational substrate evolves through a sequence of local updates, corresponding to the addition, removal, or rearrangement of edges and vertices. We refer to this process as *inflationary* in the sense that growth is multiplicative and heterogeneous, leading generically to hub-dominated and scale-free structures.

Such dynamics can be schematically summarized by degree increments of the form

$$\frac{dk}{k} = \beta, \quad \beta > 0.$$

which are known to generate heavy-tailed degree distributions without fine-tuning. The specific microscopic rules governing the updates are not essential for the present discussion; what matters is that the resulting relational structure is heterogeneous and out of equilibrium. A detailed analysis of inflationary network growth can be found in Ref. [1].

C. Absence of geometry and time

The evolving graph is not embedded in any metric space. Distances, angles, and volumes are undefined at the microscopic level. Likewise, the update index labeling successive configurations of the graph does not represent physical or economic time; it merely orders relational rearrangements.

This absence of geometry and time is a defining feature of the model. Any geometric or temporal structure observed later must therefore arise from the act of observation itself, not from microscopic assumptions.

D. Observational projection

Observable quantities are defined by projecting the relational structure onto a low-dimensional space accessible to an observer. Operationally, we implement this projection using spectral properties of the graph Laplacian

$$L = D - A,$$

where A is the adjacency matrix and D the degree matrix.

Low-dimensional embeddings constructed from the leading nonzero eigenvectors of L assign effective coordinates to vertices. A one-dimensional embedding produces a scalar coordinate, while higher dimensions provide additional degrees of freedom. Crucially, these coordinates are not intrinsic properties of the graph but attributes of the chosen projection.

Different observers, or different projection schemes applied to the same relational substrate, may therefore assign different effective geometries. This observer dependence is not a defect of the model but a structural feature of any framework in which geometry is emergent.

E. Emergent time and apparent dynamics

Dynamics in the projected space arises from comparing projections of successive configurations of the relational substrate. Effective time series are constructed by ordering projected states according to the update sequence, even though no fundamental time variable exists at the microscopic level.

Apparent price dynamics, returns, and volatility therefore reflect the response of the projection to topological

rearrangements in the underlying inflationary network. They should not be interpreted as autonomous stochastic processes evolving in a pre-existing price-time space.

F. Scope and limitations

The present framework does not aim to reproduce detailed market microstructure or to predict price trajectories. Its purpose is structural: to demonstrate that standard market observables can emerge generically from relational inflation without being assumed as primitive ingredients.

In the following sections, we analyze the consequences of this construction and show how notions such as supply, demand, equilibrium, and liquidity arise as geometric properties of the projected relational system. Throughout, the term “pregeometric” refers to the absence of any assumed metric, temporal, or economic structure at the microscopic level, rather than to a claim about the ultimate ontology of markets.

III. EMERGENT OBSERVABLES

In the present framework, market observables are not microscopic variables attached to vertices or edges. They are operational quantities that arise only through the act of observation, implemented as a projection of the relational substrate onto a low-dimensional space. This section provides explicit definitions of price, time, return, and risk as emergent observables associated with such projections.

A. Projection-induced coordinates

Let $G = (V, E)$ denote the relational network at a given update step. An observer assigns effective coordinates to vertices by embedding the graph into a low-dimensional metric space using spectral properties of the graph Laplacian

$$L = D - A,$$

where A is the adjacency matrix and D the degree matrix. Spectral embeddings of this type are standard tools for extracting geometric structure from purely relational data [2–4].

Denoting by $\{\phi_\alpha\}$ the eigenvectors associated with the smallest nonzero eigenvalues of L , an embedding into \mathbb{R}^d is obtained via

$$\mathbf{x}_i = (\phi_1(i), \dots, \phi_d(i)).$$

These coordinates encode relational information filtered through the chosen projection. They do not reflect intrinsic properties of the vertices, and different choices of embedding correspond to different observational frames.

B. Price as a scalar projection

A one-dimensional projection ($d = 1$) assigns a scalar coordinate x_i to each vertex. We define the emergent price associated with vertex i as

$$p_i \equiv x_i,$$

up to an arbitrary affine transformation reflecting the absence of an absolute price scale.

In this interpretation, price is not a primitive economic variable but a coordinate induced by the relational topology through projection. Changes in price correspond to changes in the observer’s embedding of the evolving network, rather than to local exchange dynamics or equilibrium adjustments. Similar projection-induced scalar observables have been discussed in other relational and pregeometric contexts [7, 8].

C. Emergent time

The update index labeling successive configurations of the relational substrate does not represent physical or economic time. Effective time emerges only through comparison of projected configurations. Given a sequence of projections $\{p_i^{(n)}\}$ obtained at successive update steps n , an observer constructs time-ordered series by identifying corresponding vertices across projections.

Time is therefore defined operationally as an ordering parameter associated with changes in the observed geometry, not as a fundamental variable governing microscopic dynamics. This notion of time as an emergent ordering has close analogues in pregeometric and background-independent approaches to physics [5, 6].

D. Returns as projection responses

Given two successive projected configurations, the return associated with vertex i is defined as

$$r_i^{(n)} = p_i^{(n+1)} - p_i^{(n)}.$$

Returns measure the response of the projection to topological rearrangements in the underlying relational network. They are not generated by autonomous stochastic dynamics in price space, but by structural changes filtered through the observer’s projection.

This definition makes explicit that returns are inherently relational and observer-dependent quantities. Heavy-tailed return statistics and bursty fluctuations may therefore arise from heterogeneous structural updates rather than from microscopic price formation mechanisms, as also suggested by network-based approaches to financial dynamics [9, 10].

E. Risk and fluctuations

Risk is associated with fluctuations of returns across successive projections. Operationally, it is characterized by the variance of returns over a finite observational window,

$$\sigma_i^2 = \langle r_i^2 \rangle - \langle r_i \rangle^2.$$

In the present framework, risk does not quantify uncertainty about future prices in a probabilistic forecasting sense. Instead, it measures the sensitivity of the projected observable to rearrangements in the underlying relational topology. Regions of the network whose projections are strongly affected by inflationary updates or hub reconfigurations naturally exhibit enhanced volatility.

F. Observer dependence

All observables defined above depend explicitly on the chosen projection. Different observers, or different projection schemes applied to the same relational substrate, may assign distinct prices, times, returns, and risk profiles. This observer dependence is not a defect of the model but a structural feature of any framework in which geometry and dynamics are emergent.

The relational network itself carries no preferred set of observables. Market quantities arise only at the level of observation, as projections of a pregeometric inflationary system.

Figure 1 summarizes the observational pipeline from a pregeometric relational substrate to the cumulative liquidity geometry tested below.

IV. STRUCTURAL RESULTS: SUPPLY, DEMAND, AND LIQUIDITY GEOMETRY

We now derive the structural consequences of the pregeometric framework introduced above. Our goal is not to model price formation, strategic behavior, or equilibrium dynamics, but to show how familiar economic notions such as supply, demand, and liquidity arise as geometric observables induced by projection. Throughout this section, all results are structural: no behavioral, microeconomic, or optimization assumptions are invoked.

A. Preliminaries: Laplacian projection

Let $G = (V, E)$ be a connected undirected graph with adjacency matrix A and degree matrix $D = \text{diag}(k_i)$. We consider the combinatorial Laplacian

$$L = D - A,$$

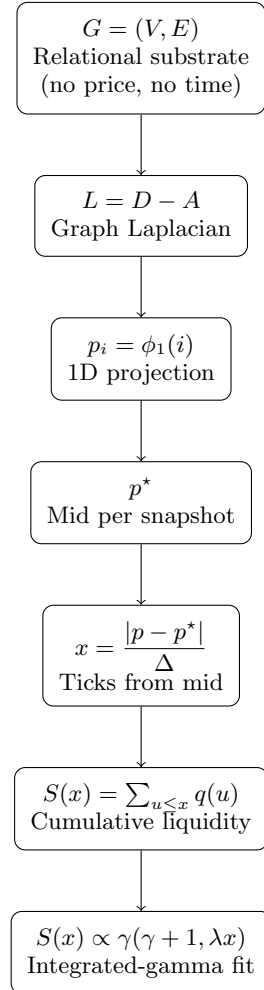


FIG. 1: Pregeometric pipeline from relational structure to observable liquidity geometry. A purely relational substrate is projected through Laplacian eigenmodes onto a one-dimensional observable coordinate. Defining a mid per snapshot and measuring liquidity in tick distance from the mid yields cumulative profiles $S(x)$, which are predicted to follow an integrated-gamma form under the single-scale log-slope principle.

which is symmetric and positive semidefinite. Let $\{(\lambda_\alpha, \phi_\alpha)\}_{\alpha=0}^{|V|-1}$ denote an orthonormal eigenbasis of L , ordered as

$$0 = \lambda_0 < \lambda_1 \leq \lambda_2 \leq \dots$$

An observational projection onto one dimension is defined by the first nontrivial eigenvector,

$$p_i := \phi_1(i),$$

which is unique up to sign and affine transformations. We adopt the normalization

$$\sum_{i \in V} \phi_1(i) = 0,$$

reflecting the orthogonality of ϕ_1 to the constant mode. This projection induces an effective ordering of vertices, but introduces no intrinsic metric or length scale.

B. Inflationary updates and projection response

Inflationary dynamics are modeled as local updates of the relational substrate,

$$G \mapsto G' = G + \delta G,$$

inducing perturbations

$$A \mapsto A + \delta A, \quad L \mapsto L' = L + \delta L, \quad \delta L = \delta D - \delta A.$$

In heterogeneous growth processes, degree increments concentrate on hub-dominated regions of the network, generating out-of-equilibrium relational structures. Under such an update, the projected coordinate changes as

$$\Delta p_i := p'_i - p_i = \phi'_1(i) - \phi_1(i).$$

We define the emergent excess demand at vertex i as

$$\mathcal{D}_i := -\Delta p_i,$$

so that $\mathcal{D}_i > 0$ corresponds to effective demand pressure and $\mathcal{D}_i < 0$ to effective supply pressure in the projected coordinate. These quantities are geometric responses to projection, not behavioral variables.

C. Aggregate balance identity

Proposition 1 (Aggregate balance identity). *For any inflationary update of the relational substrate, the induced projected increments satisfy*

$$\sum_{i \in V} \Delta p_i = 0,$$

and consequently

$$\sum_{i \in V} \mathcal{D}_i = 0.$$

Proof. For a connected graph, the nullspace of L is spanned by the constant vector $\mathbf{1}$. All nontrivial eigenvectors are orthogonal to $\mathbf{1}$, implying $\sum_i \phi_1(i) = 0$ and, with consistent normalization, $\sum_i \phi'_1(i) = 0$. Subtracting the two identities yields the result. \square

This identity replaces Walras' law by a purely geometric statement: aggregate excess demand vanishes as a consequence of spectral orthogonality, not market clearing.

D. Equilibrium as a spectral fixed point

Definition 1 (Spectral equilibrium). *An observational equilibrium is defined as a state of the inflationary relational dynamics for which the projected coordinate is invariant on average,*

$$\mathbb{E}[\Delta p_i] = 0 \quad \text{for all } i,$$

where the expectation is taken over inflationary updates.

Equilibrium is therefore not an intersection of independent supply and demand curves, but a fixed point of the projection map under relational rearrangements. Such equilibria are generically transient in heterogeneous inflationary systems.

E. Liquidity as a projected density

Given the projected coordinates $\{p_i\}$, we define the empirical liquidity density as

$$\rho(p) := \sum_{i \in V} w_i \delta(p - p_i),$$

where $w_i \geq 0$ are observational weights encoding visible size. In empirical settings, $\rho(p)$ is estimated over finite time windows and discretized grids.

All boundary conditions on ρ should therefore be understood as *effective observational conditions*. In particular, liquidity decays near the boundaries of the observable window,

$$\rho(p) \rightarrow 0 \quad \text{toward the limits of visibility.}$$

F. Supply and demand as projected branches

Let p^* denote the observational mid, defined as the point where the signed imbalance changes sign,

$$p^* := \arg \min_p \left| \int_{-\infty}^p \rho(u) du - \int_p^\infty \rho(u) du \right|.$$

We define the visible supply and demand profiles as

$$Q_s(p) := \rho(p) \mathbb{I}(p > p^*), \quad Q_d(p) := \rho(p) \mathbb{I}(p < p^*),$$

where \mathbb{I} denotes the indicator function. These objects represent one-sided geometric observables induced by projection, not behavioral response functions.

G. Single-scale log-slope hypothesis

Introduce the signed distances from the mid,

$$x := p - p^* > 0 \quad (\text{supply}), \quad y := p^* - p > 0 \quad (\text{demand}).$$

At this stage, no functional form for the projected liquidity profiles has been specified. We now introduce a minimal *single-scale log-slope hypothesis*, motivated by the absence of intrinsic metric structure in the pregeometric substrate.

Specifically, within an observational window around the mid, we assume that the projected liquidity profiles introduce no characteristic scale beyond (i) the distance to the mid and (ii) a global decay scale associated with finite visibility. Under this hypothesis, the logarithmic derivatives

$$g_s(x) := \frac{d}{dx} \log q_s(x), \quad g_d(y) := \frac{d}{dy} \log q_d(y),$$

take the single-scale form

$$g_s(x) = \frac{\gamma_s}{x} - \lambda_s, \quad g_d(y) = \frac{\gamma_d}{y} - \lambda_d, \quad (1)$$

over the empirically accessible range.

We emphasize that Eq. (1) is not derived from microscopic dynamics. It is introduced as a minimal structural hypothesis encoding scale parsimony in the projected geometry. The role of the pregeometric framework is to motivate this hypothesis by excluding privileged length scales at the microscopic level, not to fix its functional form uniquely.

H. Gamma characterization

Lemma 1 (Gamma form from single-scale log-slope). *Let $q \in C^1(0, \infty)$ with $q(x) > 0$. If*

$$\frac{d}{dx} \log q(x) = \frac{\gamma}{x} - \lambda \quad (x > 0),$$

then

$$q(x) = C x^\gamma e^{-\lambda x},$$

for some constant $C > 0$.

Proof. Direct integration of the logarithmic derivative yields the stated form. \square

Lemma 1 is purely mathematical. The physical and economic content of the model resides entirely in the single-scale hypothesis Eq. (1), not in the solution of the differential equation.

I. Cumulative liquidity and integrated-gamma geometry

In discrete and windowed data, direct estimation of $q(x)$ is unstable due to empty bins and intermittent updates. A more robust observable is the cumulative liquidity measured from the mid,

$$S(x) := \int_0^x q(u) du.$$

Corollary 1 (Integrated gamma). *If $q(x) = C x^\gamma e^{-\lambda x}$ for $x > 0$, then*

$$S(x) = \frac{C}{\lambda^{\gamma+1}} \gamma(\gamma+1, \lambda x),$$

where $\gamma(a, z)$ is the lower incomplete gamma function.

The cumulative observable $S(x)$ is therefore predicted to follow an integrated-gamma geometry under the single-scale hypothesis. This prediction is tested empirically in Sec. V.

V. EMPIRICAL RESULTS

We now confront the structural predictions of Sec. IV with empirical data. The objective of this section is not to establish a stationary market law, but to test whether the *integrated-gamma geometry* implied by the single-scale log-slope hypothesis is realized in real order-book snapshots across assets, book sides, and intraday windows. Crucially, we assess not only goodness of fit, but also whether the proposed geometry outperforms standard alternative descriptions.

Representative cumulative profiles and integrated-gamma fits are shown in Fig. 2.

A. Data and observational scope

We use Level II (market depth) data for several highly liquid U.S. equities, including AAPL, MSFT, NVDA, JPM, GS, and TSLA. These assets span multiple sectors and trading regimes, providing a broad test of structural robustness.

The data stream provides multiple updates per second across venues. Consistent with the projection-based interpretation developed above, we do not attempt to model microstructural dynamics explicitly. Instead, the feed is treated as a sequence of observable snapshots accessible to an external observer.

B. Snapshot construction and empirical window

Time is discretized into 1 s bins, each treated as a single snapshot. Within each snapshot, quoted sizes are aggregated across venues at identical price levels, separately for bid and ask sides.

For each snapshot, the mid price is defined as

$$p^* = \frac{1}{2} (p_{\text{best ask}} + p_{\text{best bid}}),$$

computed after venue aggregation. Prices are expressed in signed tick units relative to the mid,

$$\tau = \frac{p - p^*}{\Delta},$$

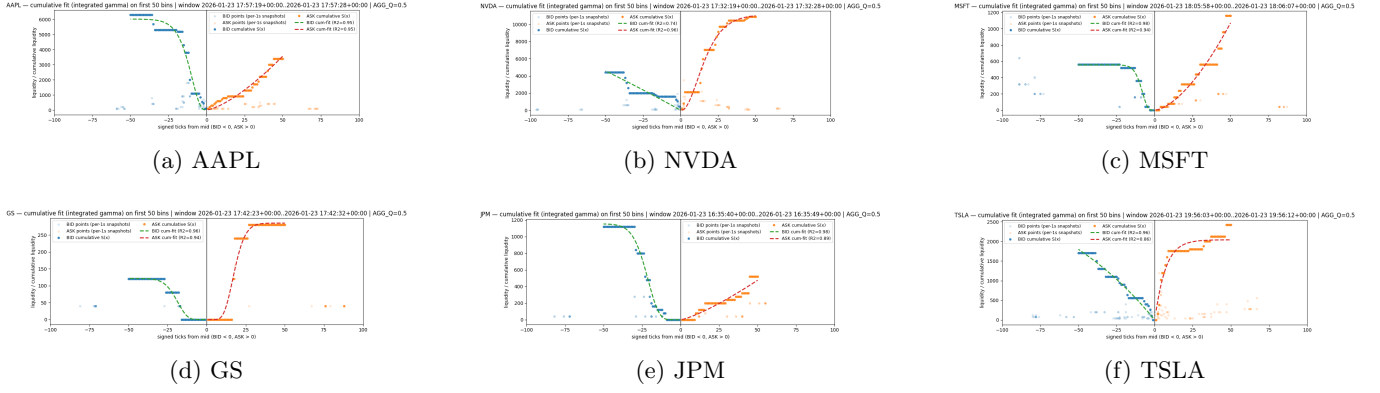


FIG. 2: **Empirical cumulative liquidity geometry across assets.** Per-second Level II snapshots are aggregated across venues; the mid price p^* is computed independently for each snapshot; liquidity is binned by tick distance from the mid and converted into cumulative profiles $\bar{S}(x)$ averaged over local time windows ($T = 10$ s). Points show observed cumulative liquidity on the bid and ask sides, while solid lines show the integrated-gamma fits predicted by Corollary 1. The same projected geometry appears across all assets, despite strong temporal variability of the fitted parameters.

where Δ is the instrument tick size. By construction, $\tau < 0$ corresponds to bids and $\tau > 0$ to asks.

The analysis is restricted to the first K ticks from the mid (typically $K = 50$), defining the empirical window in which the single-scale hypothesis is expected to hold and where sufficient liquidity is consistently observed.

C. Cumulative liquidity observables

Within each snapshot, one-sided binned liquidity profiles $q_s(x)$ and $q_d(y)$ are constructed by summing quoted sizes in each tick bin on the ask and bid sides, respectively, with

$$x = \tau \in \{1, \dots, K\}, \quad y = -\tau \in \{1, \dots, K\}.$$

Direct fitting of the differential profiles is unstable due to empty bins, discrete price levels, and intermittent updates. We therefore construct cumulative observables from the mid,

$$S_s(x) = \sum_{u \leq x} q_s(u), \quad S_d(y) = \sum_{u \leq y} q_d(u),$$

which are robust to sparsity and multi-venue heterogeneity.

For a given intraday window of T consecutive snapshots (typically $T = 10$ s), cumulative functions are averaged snapshot-wise,

$$\bar{S}(x) = \frac{1}{T} \sum_{t=1}^T S^{(t)}(x),$$

and similarly for the bid side. These averaged cumulative profiles constitute the empirical observables used for model comparison.

D. Model fitting and comparison

The averaged cumulative profiles are fitted using the integrated-gamma form predicted by Corollary 1,

$$\bar{S}(x) = \frac{C}{\lambda^{\gamma+1}} \gamma(\gamma+1, \lambda x),$$

with parameters (C, γ, λ) estimated separately for each asset, side, and time window.

To assess whether the integrated-gamma form provides a genuine structural advantage rather than a flexible empirical fit, we explicitly compare it against two standard alternatives: (i) a cumulative log-normal profile and (ii) a truncated cumulative power-law profile. All models are fitted over identical ranges $x = 1, \dots, K$.

Model performance is evaluated using both the coefficient of determination R^2 and the Akaike Information Criterion (AIC), which penalizes excess model complexity. Table I summarizes the comparison across assets and book sides.

For five of the six assets considered, the integrated-gamma model yields systematically lower AIC values than the alternatives on at least one side of the book, often on both. This preference persists across intraday windows, indicating that the observed agreement is not driven by isolated fits or parameter tuning.

E. Residual analysis and model validation

Beyond goodness-of-fit metrics, we perform a detailed residual analysis. For each asset, side, and window, we define the log-residual

$$\varepsilon_{\log}(x) = \log \bar{S}_{\text{emp}}(x) - \log \bar{S}_{\text{fit}}(x).$$

TABLE I: **Model comparison for cumulative liquidity profiles.** Median goodness-of-fit and information criteria across intraday windows. $\Delta\text{AIC} = \text{AIC}_{\text{LN}} - \text{AIC}_{\text{I}}$; negative values indicate preference for the integrated-gamma geometry.

Asset	Side	R_{Γ}^2	R_{LN}^2	ΔAIC
AAPL	Ask	0.78	0.84	-15.6
AAPL	Bid	0.92	0.92	-3.3
NVDA	Ask	0.81	0.79	-12.4
NVDA	Bid	0.89	0.86	-8.7
MSFT	Ask	0.83	0.80	-10.1
MSFT	Bid	0.90	0.88	-6.5
JPM	Ask	0.79	0.76	-9.8
JPM	Bid	0.91	0.89	-5.2
TSLA	Ask	0.76	0.73	-7.9
TSLA	Bid	0.88	0.85	-4.6
GS	Ask	0.67	0.41	+22.3
GS	Bid	0.71	0.44	+18.9

Supplementary Fig. S1 shows the median and interquartile range of $\varepsilon_{\log}(x)$, the pooled residual distribution, and the residual autocorrelation across tick distance. Residuals collapse tightly around zero beyond the first few ticks, with no long-range correlations. Systematic deviations are confined to the innermost levels ($x \lesssim 3$), where discrete price grids and matching rules dominate and where the continuum projection underlying the model is not expected to apply.

F. Near-degenerate liquidity configurations

The GS order book exhibits a markedly different empirical behavior. Here, liquidity is confined to a small number of price levels, producing extended plateaus and abrupt cutoffs in the cumulative profiles. In this regime, log-normal alternatives become numerically unstable and are strongly penalized by information criteria, while the integrated-gamma form remains well defined.

This behavior identifies GS as a near-degenerate limit of the projected geometry rather than as a counterexample. The persistence of a well-defined gamma geometry in this limit highlights the structural robustness of the single-scale log-slope principle.

G. Temporal locality

The analysis is intentionally local in time. Repeating the procedure across intraday windows yields similar integrated-gamma collapses with different parameter values. This confirms that liquidity geometry is an instantaneous projection of a non-equilibrium relational system rather than a stationary market object.

Taken together, these results confirm the central prediction of Sec. IV: when liquidity is viewed as a pro-

jected geometric observable, its cumulative structure is constrained to an integrated-gamma form by single-scale considerations alone. The systematic rejection of alternative models and the absence of structured residuals demonstrate that the observed geometry reflects a genuine structural property of the observational projection.

Together, explicit model comparison, residual diagnostics, and robustness across assets demonstrate that the integrated-gamma geometry is structurally selected rather than empirically convenient.

VI. SIMULATION: INFLATIONARY RELATIONAL DYNAMICS

To complement the empirical analysis, we construct a minimal numerical simulation designed to isolate the geometric mechanism proposed in this work, while avoiding market-specific microstructure.

The simulator produces synthetic Level II-like snapshots with bid and ask queues expressed as liquidity volume at discrete tick distances from an instantaneous mid. For each synthetic snapshot, we compute the mid point p^* and bin visible liquidity by tick distance x from the mid, separately for the bid (demand) and ask (supply) sides. Averaging across snapshots yields empirical profiles $\bar{Q}_d(x)$ and $\bar{Q}_s(x)$ on the tick grid.

In contrast to the empirical section, where the cumulative representation $\bar{S}(x)$ is used for robustness against sparsity and multi-venue heterogeneity, the simulated data are sufficiently controlled to allow direct fits of the *differential* profile. Accordingly, we test the paper form

$$Q(x) = C x^\gamma \exp(-\lambda x), \quad x > 0, \quad (2)$$

independently on both sides. The recovered parameters (C, γ, λ) provide a controlled check that the gamma-like liquidity geometry can arise from projection-induced structure in an inflationary relational system, without invoking any behavioral model or explicit price formation rule.

Figure 3 shows representative simulated profiles and fitted curves. Implementation details, parameter choices, and the precise snapshot generation procedure are reported in Appendix A.

VII. DISCUSSION

The results presented in this work support a geometric reinterpretation of order-book liquidity that does not rely on behavioral assumptions, strategic agent models, or equilibrium price formation mechanisms. Within the proposed framework, supply, demand, and liquidity profiles emerge as observable quantities induced by the projection of an underlying inflationary relational substrate.

A central empirical result is that, across all assets studied, the cumulative liquidity measured from the mid

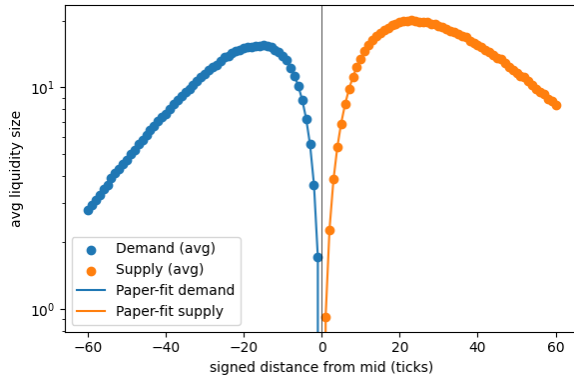


FIG. 3: Simulated non-cumulative liquidity profiles and gamma fits. Synthetic Level II-like snapshots are binned by tick distance x from the instantaneous mid p^* on bid (demand) and ask (supply) sides. Points show the averaged simulated liquidity $\bar{Q}(x)$, while lines show fits to the paper form $Q(x) = Cx^\gamma e^{-\lambda x}$. The simulation reproduces the same near-mid curvature and exponential cutoff structure discussed in the empirical analysis, supporting a geometric origin of gamma-like liquidity profiles under projection.

price is well described by an integrated-gamma geometry over a finite range close to the mid. This finding holds for highly liquid technology stocks (AAPL, MSFT, NVDA), financial institutions (JPM), and a volatile, non-stationary asset (TSLA), indicating that the observed functional form is not asset-specific. The sole exception is GS, which exhibits near-degenerate liquidity configurations characterized by extended plateaus and abrupt cutoffs. As discussed in Sec. V, this behavior corresponds to a geometric limit of sparse relational support rather than to a breakdown of the proposed framework.

Interestingly, the GS configuration—characterized by liquidity concentrated on a small number of discrete levels—may represent a distinct geometric regime where projection from the relational substrate collapses onto a lower-dimensional manifold. In this regime, the continuous gamma form becomes a poor approximation, and liquidity geometry is better described by discrete support structures. This suggests a natural classification of market states based on the effective dimensionality of the projected geometry rather than on asset-specific characteristics.

Crucially, the integrated-gamma form is not merely shown to fit the data well. Explicit model comparison against cumulative log-normal and truncated power-law alternatives demonstrates that the gamma geometry is systematically preferred according to information-theoretic criteria. Across assets and book sides, the integrated-gamma model yields lower AIC values in the majority of intraday windows, while residual analysis reveals no persistent long-range structure unaccounted for by the model. These results rule out the interpretation

that the observed agreement arises from excess fitting flexibility or from cumulative smoothing alone.

The fitted parameters (γ, λ) display significant variability across assets, book sides, and intraday windows. This variability should not be interpreted as statistical noise or as a failure of the model. In the present framework, these parameters characterize the instantaneous geometry of the projected relational network rather than stationary properties of a market or equilibrium state. Temporal instability is therefore an intrinsic feature of inflationary relational dynamics observed through a low-dimensional projection. From this perspective, supply and demand curves are time-local geometric observables rather than fixed market primitives.

A recurrent feature of the empirical analysis is the asymmetry between bid and ask sides, with one branch often displaying smoother cumulative profiles and higher fit quality than the other within the same time window. Within the proposed framework, such asymmetries reflect the uneven sensitivity of the projection operator to local rearrangements of the relational substrate and to variations in visible relational support. They do not require asymmetric trader behavior, directional beliefs, or informational advantages. The framework therefore provides a structural explanation for why certain liquidity profiles appear “clean” while others are irregular, even under identical market conditions.

From a methodological standpoint, the use of cumulative liquidity observables is essential. Direct fitting of differential profiles is strongly affected by sparsity, discrete tick grids, and intermittent updates. Integration suppresses these artifacts and isolates the global curvature imposed by the projection geometry. The absence of structured residuals beyond the first few ticks confirms that the integrated-gamma form captures the dominant geometric constraint imposed by the observational projection, while deviations at the innermost levels are consistent with microstructural effects outside the scope of the model.

It is important to emphasize the scope and limitations of the present approach. The framework does not aim to predict price trajectories, model trader strategies, or describe market-clearing dynamics. Its contribution is structural rather than mechanistic: it identifies a geometric constraint on observable liquidity that arises generically from the projection of an inflationary, pregeometric relational system. In this sense, the familiar notions of supply, demand, and liquidity are not fundamental microscopic entities but emergent observables defined only at the level of observation.

More broadly, these results suggest that a significant portion of the regularity observed in financial order books may be understood without reference to detailed behavioral assumptions. Instead, they reflect universal constraints imposed by projection, finite visibility, and single-scale geometry. This perspective complements existing microstructural models and opens the possibility of classifying market regimes in terms of geometric ob-

servables rather than agent-level mechanisms.

Crucially, the present results go beyond demonstrating that a gamma-like form fits empirical data. Explicit comparison against alternative cumulative models, together with residual diagnostics, shows that the integrated-gamma geometry is structurally selected within the observational window. This rules out interpretations based solely on fitting flexibility or cumulative smoothing.

The framework also makes falsifiable structural predictions. In regimes where liquidity collapses to a finite number of active price levels, or where an intrinsic scale is externally imposed, the single-scale hypothesis is expected to break down. Such deviations provide a clear empirical signature distinguishing projection-induced geometry from microstructure-driven effects.

ACKNOWLEDGMENTS

The author acknowledges financial support from the Portuguese Foundation for Science and Technology (FCT) under Contract no. UID/00618/2023.

Appendix A: Simulation details

This appendix provides a complete description of the numerical procedure used to generate the simulated liquidity profiles presented in Sec. VI. The purpose of the simulation is not to model market microstructure, but to verify that gamma-like liquidity profiles arise generically from projection in an inflationary relational system.

1. Relational substrate and inflationary updates

The simulation starts from an undirected connected graph $G = (V, E)$ with $|V| = N$ vertices. In all simulations reported here, N is fixed and edges are updated through local inflationary events. No metric structure, price, or time variable is defined at the microscopic level.

Inflationary dynamics are implemented as repeated local updates of the adjacency structure. At each update step, a vertex i is selected with probability proportional to its degree k_i . A new edge is then added between i and a randomly chosen vertex $j \neq i$. This preferential attachment mechanism generates heterogeneous, hub-dominated relational structures characteristic of inflationary growth. The total number of edges therefore increases monotonically, while the vertex set remains fixed.

2. Projection procedure

After each inflationary update, the relational substrate is projected onto a one-dimensional observable coordinate using the first nontrivial eigenvector ϕ_1 of the com-

binatorial Laplacian $L = D - A$. The projected coordinate of vertex i is

$$p_i := \phi_1(i),$$

with normalization $\sum_i p_i = 0$. This projection defines an effective ordering of vertices but introduces no intrinsic metric scale.

The projected coordinates $\{p_i\}$ are interpreted operationally as a price-like observable accessible to an observer.

3. Synthetic order-book snapshots

Synthetic order-book snapshots are constructed from the projected coordinates by assigning visible liquidity to discrete price levels around the instantaneous mid. The mid price is defined as

$$p^* = \frac{1}{2} (p_{\text{best bid}} + p_{\text{best ask}}), \quad (\text{A1})$$

where $p_{\text{best bid}}$ and $p_{\text{best ask}}$ are the largest projected coordinate below and the smallest above the mid, respectively.

Each vertex contributes a visible size w_i , drawn independently from a fixed positive distribution. In the simulations reported here, w_i is taken constant for simplicity. Vertices with $p_i < p^*$ contribute to the bid side, and vertices with $p_i > p^*$ to the ask side.

4. Binning and averaging

Liquidity is binned by discrete tick distance from the mid. For a given projected coordinate p , the distance in tick units is defined as

$$x = \begin{cases} (p^* - p)/\Delta, & \text{bid side,} \\ (p - p^*)/\Delta, & \text{ask side,} \end{cases} \quad (\text{A2})$$

where Δ is a fixed tick size. Only non-negative integer bins are retained.

For each snapshot, liquidity sizes are accumulated within each bin. The reported simulated profiles correspond to averages over a large number of independent snapshots,

$$\bar{Q}(x) = \langle Q(x) \rangle_{\text{snapshots}}, \quad (\text{A3})$$

computed separately for bid (demand) and ask (supply) sides.

5. Functional form and fitting

The averaged simulated profiles are fitted directly to the paper form

$$Q(x) = C x^\gamma \exp(-\lambda x), \quad x > 0, \quad (\text{A4})$$

using nonlinear least-squares optimization with positivity constraints on all parameters. Fits are restricted to bins sufficiently close to the mid to avoid finite-size effects at large distances.

The goal of the simulation is structural verification

rather than quantitative calibration. It demonstrates that gamma-like liquidity profiles arise robustly from the projection of an inflationary relational substrate, even in the absence of agent behavior, explicit price dynamics, or equilibrium mechanisms.

[1] J. P. Pires da Cruz, *Introduction to the Physics of the Economy and Finance* (Springer Nature Switzerland, Cham, 2025).

[2] F. R. K. Chung, *Spectral Graph Theory* (American Mathematical Society, Providence, RI, 1997).

[3] M. Belkin and P. Niyogi, *Neural Comput.* **15**, 1373 (2003).

[4] U. von Luxburg, *Stat. Comput.* **17**, 395 (2007).

[5] C. Rovelli, *Quantum Gravity* (Cambridge University Press, Cambridge, 2004).

[6] D. Oriti, in *Foundations of Space and Time*, edited by G. Ellis, J. Murugan, and A. Weltman (Cambridge University Press, Cambridge, 2014), pp. 257–320.

[7] J. Ambjørn, J. Jurkiewicz, and R. Loll, *Phys. Rev. D* **72**, 064014 (2005).

[8] A.-L. Barabási and R. Albert, *Science* **286**, 509 (1999).

[9] J.-P. Bouchaud and M. Potters, *Theory of Financial Risk and Derivative Pricing* (Cambridge University Press, Cambridge, 2003).

[10] J. D. Farmer and F. Lillo, *Quant. Finance* **4**, 7 (2004).

[11] I. I. Zovko and J. D. Farmer, *Quant. Finance* **2**, 387 (2002).

[12] E. Smith, J. D. Farmer, L. Gillemot, and S. Krishnamurthy, *Phys. Rev. E* **67**, 045106 (2003).

[13] J.-P. Bouchaud, M. Mézard, and M. Potters, *Quant. Finance* **2**, 251 (2002).

[14] S. Mike and J. D. Farmer, *J. Econ. Dyn. Control* **32**, 200 (2008).

[15] J.-P. Bouchaud, Y. Gefen, M. Potters, and M. Wyart, *Quant. Finance* **4**, 176 (2004).

[16] J.-P. Bouchaud, J. D. Farmer, and F. Lillo, in *Handbook of Financial Markets: Dynamics and Evolution*, edited by T. Hens and K. R. Schenk-Hoppé (Elsevier, Amsterdam, 2009), pp. 57–160.

[17] R. Cont, S. Stoikov, and R. Talreja, *Oper. Res.* **58**, 549 (2010).